Evaluation of Impurity Composition and Content in the TAL at Various Operating Regimes

IEPC-2005-147

Presented at the 29th International Electric Propulsion Conference, Princeton University, October 31 – November 4, 2005

G.F. Karabadzhak*, A.V. Semenkin†, A.E. Solodukhin‡ and O.S.Tverdokhlebov§
Central Research Institute of Machine-Building (TSNIIMASH), Korolev, Moscow region, 141070, Russia

Abstract: The paper is dedicated to development and validation of a real time optical diagnostic method for monitoring of the Hall effect thruster erosion rate variation from one operating regime to another. A convenient semi-empirical formula has been utilized for relation of the thruster erosion rate with intensities of the impurity and xenon emissions. The formula was verified in a number of dedicated experiments. In particular, the erosion rate predictions based on the optical diagnostic data were compared with results of the thruster ware tests. Good agreement has been found. Additional verification of the method was achieved through measurements of variation of the erosion rate coefficient of metallic samples placed inside the ionic beam in the Hall thruster plume. The method was found to be appropriate for measuring of the erosion rate variation in a wide range of the thruster operating parameters. However, some limitations of the method have been manifested. In particular, evaluation of the erosion rate variation becomes less accurate, when electron temperature in the thruster plasma varies from one operating regime to another. In this case formula for the erosion rate variation must be generalized to include dependence of the emission excitation functions on the electron temperature.

Nomenclature

A	=	spontaneous radiation decay probability
n_e	=	electron number density
N_s	=	impurity specie atomic number density
N_+	=	xenon first ion number density
R	=	thruster erosion rate
$\sigma_{pi}(\varepsilon)$	=	particle specific, i-th level electron collision excitation cross-section
$Q(T_e)$	=	emission excitation function
I_s	=	emission intensity of impurity atoms
I_+	=	emission intensity of xenon ions
k_s	=	sputter coefficient
U	=	thruster operating voltage
j_+	=	ion beam current density

I. Introduction

DETERMINATION of the impurity atom content in xenon propelled EP thruster plasma is continuously addressed with regard to evaluation of the thruster operating time resources. The impurities result from erosion

* Head of Laboratory, Heat Exchange Center, karabadzhak@tsniimash.ru.
† Head of Laboratory, Electric Propulsion Lab., avs@tse.ru.
‡ Group Leader, Electric Propulsion Lab., asolodukhin@mtu-net.ru.
§ Research Engineer, Electric Propulsion Lab., olekos@infoline.su.

of the thruster body elements and therefore their content in the plasma can be directly related to the thruster erosion rate. Extended overview of optical methods for measurement of ion thrusters grid erosion rate was given in Ref.1. These methods are really promising, because they do not intrude the plasma and because they offer evaluation of the erosion rate in a real time. Optical spectroscopic method, which is based on analysis of the plasma emission spectra, is often applied in practice. Main problem of this method is to relate intensity of the impurity emissions with number densities of the impurity atoms and with the thruster erosion rate. This relation is not always straight and obvious. Generally, a Collisional-Radiative Model (CRM) has to be introduced to implement this relation. However, development of accurate CRM in rarified plasma of xenon operating thrusters represent substantial problem[2]. Under these circumstances a convenient semi-empirical model for evaluation of the impurity atom content in rarified xenon plasma was suggested earlier[3]. The model assumes that emissions of xenon and impurity species are induced by pure electronic collisions and, so that they may be expressed as:

$$I_{ik} = \frac{A_{ik}}{\sum_{r<i} A_{ir}} h\nu_{ik} n_e N_p \langle \sigma_{pi} v_e \rangle = C_{pik} n_e N_p \langle \sigma_{pi} v_e \rangle \tag{1}$$

where A – spontaneous radiation decay probability; $h\nu$ - photon energy; n_e – electron number density; N_p – plasma specie atomic number density; $\sigma_{pi}(\varepsilon)$ – particle specific, i-th level electron collision excitation cross-section, which depends on the electron energy; brackets mean averaging over the electron velocity $\mathbf{v_e}$ distribution function; C_{pik} – particle and level specific constant.

Obviously, C_{pik} doesn't depend on the thruster operating mode, so that variation of any particular emission intensity should be a product of variations of the number densities n_e, N_p and excitation function $Q_{pi}(T_e)=<\sigma_{pi}v>$, which depends on the electron temperature. Considering ratio of any sputtered impurity emission intensity I_s to a xenon ionic emission intensity I_+ and assuming direct proportionality between thruster erosion rate R and the sputtered impurity atom number density N_s, simple relation for evaluation of the erosion rate variation was reduced in Ref.3:

$$\delta R = \delta N_+ \cdot \frac{\delta I_s}{\delta I_+} \cdot \frac{\delta Q_+(T_e)}{\delta Q_s(T_e)} \tag{2}$$

turning into

$$\delta R \approx \delta N_+ \cdot \frac{\delta I_s}{\delta I_+} \tag{3}$$

at the condition when ratio of the excitation functions $\frac{Q_s}{Q_+}$ doesn't vary much from one operating mode to another.

These relations provided a basis for a new optical method of the thruster erosion rate evaluation. Attractive feature of the new method was that erosion rate could be measured almost in a real time, whereas even accelerated direct measurement of the thruster body erosion properties require from tens to hundreds hours of the thruster ware tests. Preliminary tests of the new optical method on a Thruster with Anode Layer (TAL) revealed fairly promising results[4]. Recently similar method was applied for studying of the erosion rate variation in a Hall Effect Thruster (HET) of SPT (Stationary Plasma Thruster) type[5]. Relation (3) was utilized in these works, despite that it wasn't completely validated. Furthermore, as it was found out during the current study, relation (3) appeared to be not sufficiently accurate at some plasma conditions and therefore more general formula (2) should be applied. General problem with application of this formula is that variation of the excitation function ratio $\frac{Q_s}{Q_+}$ can't be easily monitored. Neither it can be easily predicted. Therefore, utilization of simplified formula (3) is more preferable when possible. Extended research has been undertaken to understand when the optical method for evaluation of the erosion rate variation based on relation (3) is applicable and when more general equation (2) should be applied. Present paper documents results of this research and suggests its future development.

II. Experimental Setup

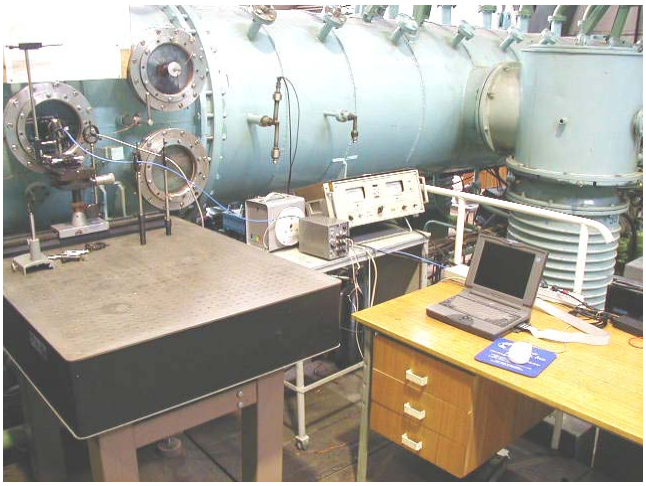

Figure 1. TSNIIMASH facility #2 and diagnostic equipment during measurement of the SETAL erosion properties.

Most of the verification tests of the new optical method for evaluation of the impurity content in the HET plasma were conducted on a specialized D80-type laboratory TAL, conventionally named Specialized Experimental TAL (SETAL). The thruster could operate both in single and double stage mode. Operating conditions of the thruster easily varied in a wide range, providing excellent capability for comprehensive verification of the new diagnostic method and studying of its limitations. Guard rings of this thruster were made from stainless steel, but could also be easily replaced with other materials, such as carbon and ceramics. All tests were conducted on TSNIIMASH test facility #2. The facility had a quartz window, which allowed the plasma spectra acquisition in a wide spectral region from UV to NIR. The window was equipped by a shutter that prevented its sputtering by the impurity atoms during long duration tests. In most tests a CCD based spectrometers were used for the measurements. When the plasma radiation was too weak a more powerful quartz monochromator followed by a photo-multiplier was utilized. Radiation was delivered to the entrance slits of the spectral devices through optical cable. Generally, the optical systems allowed spectral resolution $\Delta\lambda$~0.1-0.2 nm in the UV and visible spectral regions and $\Delta\lambda$~0.5-1.5 nm in the NIR region. Most of the spectra were acquired from the discharge region where concentration of the sputtered impurity atoms was maximal. Spatial resolution in these measurements was 7-10 mm. Picture of the test facility and diagnostic equipment is shown in Figure 1.

III. Results and discussion

A. Identification of the impurity emission lines in the TAL spectra

At the first stage of the research numerous TAL emission spectra available in TSNIIMASH were analyzed and impurity lines were identified in those spectra. As expected, most of the impurity emissions represented components of the TAL guard ring and magnetic system poles materials, because these parts of the thruster are maximally exposed by the ionic beams. For the guard ring made from stainless steel and magnetic poles made from permendure most intense lines represented emissions of chrome, iron and cobalt. Molybdenum emissions were also found at the close vicinity of cathode-neutralizer. In case when the thruster's guard ring or discharge chamber walls were made from ceramics boron and silicon emissions could be found in the discharge plasma spectrum. To elaborate identification of the impurity lines a set of dedicated experiments was conducted. At those experiments samples of typical materials of the thruster body were put into the energetic ion beam in the TAL plume (Figure 2). The ions caused intensive sputtering of the samples accompanied by luminescence of the sputtered atoms. Comparison of the luminescent spectra with those taken from the TAL discharge provided direct way to identification and further analysis of the impurity emissions. Figure 3 illustrates this comparison.

Figure 2. Samples of materials in the TAL beam.

Table 1 summarizes the emissions, which were observable in the beam experiment spectra.

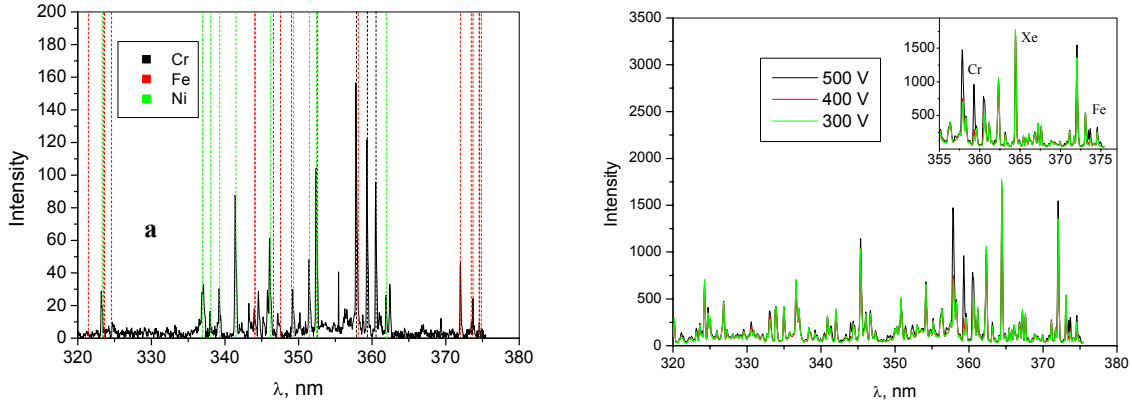

Figure 3. Spectra of the SETAL plume taken from the sample of stainless steel located inside the ionic beam (a) and from the SETAL discharge at different operating voltages (b).

Among variety of the impurity emissions those atomic lines were selected for further analysis, which might be easily separated from neighbor xenon emissions by an ordinary, not very powerful, spectral device. For comprehensive verification of the new method for the erosion rate evaluation and definition of limitations of Equation (3) dedicated experiments were carried out. In most of these experiments erosion rate was evaluated through analysis of CrI 359.3 nm, FeI 248.33-248.98 nm and Xe II 364.4 and 247.6 nm emissions.

Table 1. Impurity emission lines, which may be utilized for evaluation of the SETAL erosion rate.

Element	Wavelengths of diagnostic lines, nm
Cr	357.868, 359.348, 360.532 425.433, 427.481, 428.973 520.451, 520.602, 520.842
Fe	246.26, 248.33, 248.81, 248.98, 252.29, 252.75, 260.68, 271.9, 272.09, 273.36,273.73, 274.24, 274.4, 275.01, 275.57, 296.69, 297.01, 297.32, 298.36, 299.44, 300.1, 302.06, 303.74, 304.76, 305.74, 305.91, 318.08, 318.49, 319.17, 321.44323.46, 323.62, 324.6, 344.06, 344.1, 346.59, 347.55, 349.06, 352.6, 358.12, 371.99, 373.49, 373.71, 374.56, 374.59, 374.83, 382.04, 382.59, 385.99, 404.58, 406.36, 427.18, 430.79, 432.58, 438.35, 440.48
Co	240.73, 241.16, 242.49, 243.22, 304.4, 340.51, 341.23, 343.16, 345.35, 346.58 350.23, 350.98, 351.04, 351.26, 351.35, 351.84, 352.16, 352.34
Ni	228.71, 300.25, 305.08, 310.2, 313.41, 323.3, 336.96, 338.06, 339.3, 341.48 346.16, 349.3, 351.5, 352.45 361.94
Si	250.69, 251.43, 251.61, 252.41, 252.85, 288.16, 390.55
B	249.68, 249.77

B. Validation of the new optical method

1. Validation of the optical diagnostic method through comparison with results of direct ware tests

Direct validation of the new optical diagnostic method for evaluation of the TAL erosion rate was carried out through comparison of the optical diagnostic data with results of the thruster ware tests. Guard rings of the SETAL were made from stainless steel in those tests accelerating the test substantially. Therefore, chrome and iron emissions, in particular, were found in the SETAL discharge plasma spectrum. Three consecutive ware tests each of about 30 hours duration were implemented. The thruster operated in three different modes in those tests: high-voltage, double-stage and high-current. All operating parameters of the thruster, such as voltage, current, flow rate etc were preset specifically for each operating regime and stayed constant during particular tests. The plasma spectra were taken once per 0.5-1 hour and relative variation of the erosion rate was calculated through Equation (3). A

number of CrI and FeI emissions were utilized for computation of the erosion rate variation. Figure 4 illustrates how sensitive is the result to the choice of impurity and reference xenon lines.

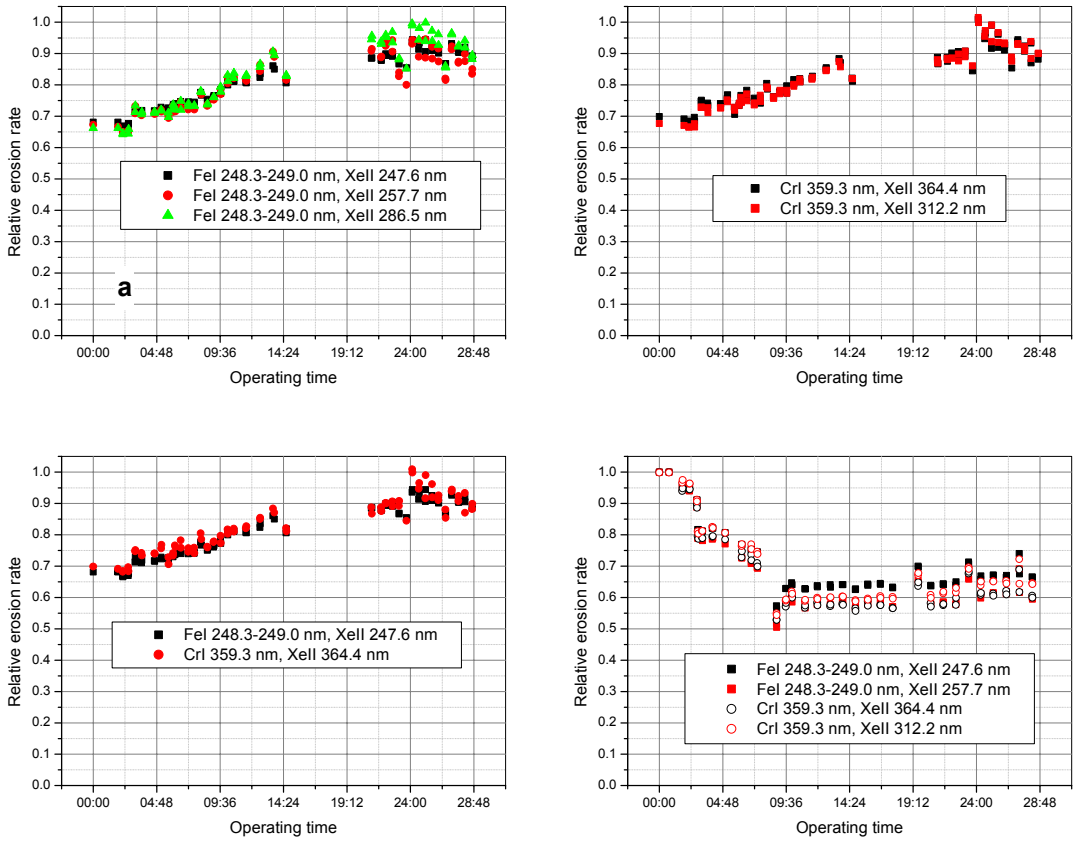

Figure 4. Measurement of the SETAL erosion rate relative variation during the thruster ware tests: a)-c) - high voltage mode, d) - double stage mode. Legend shows the lines used in the erosion rate computation.

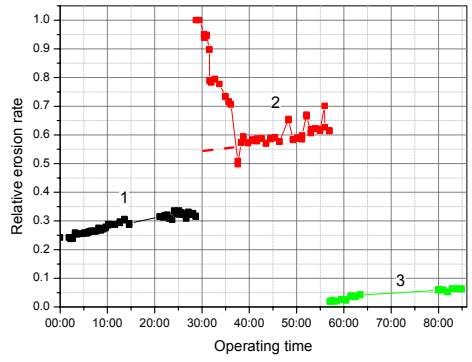

Figure 5. Erosion rate variation throughout three consecutive ware tests: 1 – high-voltage, 2- double-stage, 3 – high-current.

Evidently, that all normalized curves demonstrate almost similar variation in time. Two important conclusions can be derived from these tests: i) if operating condition doesn't change much during a test, the optical method is not very sensitive to the choice of impurity and xenon lines utilized for the erosion rate evaluation and ii) different components of the stainless steel are sputtered with the same rate. The latter conclusion has also been stated in Ref.6.

Figure 5 illustrates the erosion rate variation throughout all tree tests. Obviously, overall behavior of the optically measured erosion rate variation in this figure is in a qualitative agreement with general erosion properties of the plasma thrusters: it is bigger at higher operating voltage and yet more bigger in the double-stage regime in comparison with the high-current (lower voltage) operating mode. The erosion rate variation curves were integrated over the test duration times, providing total erosion values in relative units. After each test the guard ring ablation was measured by a high precision

profile-meter and thickness of the guard ring walls was determined with accuracy of 0.02 mm. Integral erosion data obtained from optical measurements were compared with the normalized measurements of the guard ring ablation. The guard ring ablation measurements and integral measurements of the erosion rate by optical method may be compared in columns 2 and 3 of Table 2.

As one may notice the curves in Figure 5 have the same trend, except the part on the double-stage curve between 30^{th} and 38^{th} hrs. Evidently that inclusion of the additional part of the discharge chamber in the double stage mode raised up the erosion rate somehow. A hypothesis was suggested that part of the impurity atoms sputtered the first stage chamber walls during preceding operation, so that first hours of the operation in the double stage mode are characterized both real erosion of the second stage (guard rings) and apparent erosion of the first stage (sputter of previously deposited matter). Note that the first stage originally doesn't include stainless steel components. The hypothesis was proved in dedicated experiments. At those experiments the SETAL operated in a double stage mode with stainless steel guard rings in the second stage. After that carbon rings substituted the guard rings, so that no iron and chrome atoms should be expected in the discharge. Nevertheless, some amount of chrome persisted in the plasma even after replacing of the guard ring material. Intensity of the chrome lines correlated with the first stage operating voltage, thus indicating where the impurity came form.

As soon as the direct measurements of the thruster ablation didn't include the first stage elements, earlier part of the double-stage curve in Figure 5 should be corrected through extrapolation of the later one, as it is shown in the figure by the dashed line. This correction affects the integrals as well. So, corrected values of the integrals are presented in Table 2 too.

As Table 2 demonstrates results of both direct and optical measurements of the erosion rate variation from one regime to another are in a good agreement, indicating good capabilities of the optical method.

In contrast to the ware tests, where average in time erosion rate may be determined only after tens and even hundreds hours of thruster operation, optical method is capable to measure relative erosion rate in a real time. Figure 5 shows that erosion rate didn't stay constant during the tests. While the decrease of the erosion rate observed within first 7-8 hours of the SETAL operation in the double-stage regime was explained by the first stage effect, other particularities of the double stage curve behavior required further analysis. Abrupt drops of the erosion rate curve around 32^{nd} and 35^{th} hours appeared right after tuning of the magnetic field configuration. Small rises of the erosion rate curve between 45^{th} and 55^{th} hours appeared right after temporal termination of the thruster operation followed by a new switching on. At the moment of the ware tests completion it was not clear whether these short-timescale variations of the erosion rate were actually true or reflected inaccuracy of the measurements and limitation of relation (3), in particular. To achieve thorough validation of the new method, parametric dependence of the SETAL erosion rate behavior was studied.

Table 2. Comparison of the SETAL guard ring ablation measurement with integral erosion rate variation obtained from spectroscopic measurements.

Mode	Relative erosion from the wall profile	Relative erosion from The optical diagnostics	Relative erosion from optical diagnostics (corrected)
Double stage	1	1	1
High voltage	0.58	0.45	0.51
High current	0.070	0.072	0.080

2. Validation of the Optical Diagnostic Method Through Measurement of a Sample Sputter Coefficient Variation at Different Ionic Energies in the TAL Plume

It is well known, that main cause of the thruster body ablation is energetic ions coming from the discharge plasma and hitting the discharge chamber (guard ring) walls. With growth of the operating voltage energy of the ions in the HET plasma also grows. Because xenon ion impact sputter coefficients of all materials are growing functions of energy[6], one should generally expect increase of the thruster erosion rate with increase of its operating voltage. Numerous SETAL tests proved this supposition. The erosion rate variations reflected the sputter coefficient dependences on a qualitative level. However, substantial deviation was also evident at some voltages. In fact, erosion rate is proportional to both the sputter coefficient and total ion flux intensity hitting the thruster walls. These parameters are, apparently, affected by such factors like the wall temperature and surface condition, ion beam divergence and charge composition etc, which, in turn, may vary from one operating regime to another. So, deviations of the erosion rate curve from the sputter coefficient energy dependence might be attributed to variation

of these factors. It is not easy to control all these parameters in the TAL discharge. Much easier these parameters may be controlled in the TAL plume. Most substantial effect of the discharge voltage variation onto the plume parameters is that ion beam velocity changes almost proportionally to the voltage square root. Other parameters, which might influence the optical method results, such as propellant utilization factor, plume divergence, electron temperature in the plume, relative composition of the first ion doesn't change much with variation of the voltage in the region 200-500 V[7]. So, for the samples installed inside the TAL plume, energy dependence of the sputter coefficients may be reduced from Equation (3) as follows:

$$\delta k_s = \frac{\delta R}{\delta j_+} \approx \frac{\delta N_+}{\delta j_+} \cdot \frac{\delta I_s}{\delta I_+} = \delta\sqrt{U} \cdot \frac{\delta I_s}{\delta I_+} \tag{4}$$

where k_s – sputter coefficient; U – operating voltage; j_+ - ion beam current density; δ - is operator for variation of the respected parameter, representing ratio of the parameter value at the moment to its initial value.

Intensities of the Cr lines were measured for samples of stainless steel inserted into the TAL plume at the distance of about 50 cm from the thruster. The sputter coefficient variation was reduced from these measurements through Equation (4). Measured coefficient is compared with literature data[6] in Figure 6. Black squares in the figure represent the sputter coefficient reduced directly form equation (4) and normalized to the absolute value of the data from Ref.6. Small discrepancy in the slope of the curves is noticeable in the figure. Most probably, this discrepancy results from the small reduction of the ion beam divergence with the operating voltage increase. Due to this factor the ion beam cross-section slightly reduces and ion flux density at the sample surface increases. The ion current distribution in the plume was measured by a Faraday cup probe and effect of the current distribution narrowing was evaluated. A correction coefficient, which accounts for variation of the ion flux density, has been introduced into Equation (4) and sputter coefficient has been reduced from the measurements basing on the improved formula. Red circles in Figure 6 represent corrected energy dependence of the sputter coefficient. Excellent agreement between measured and literature data is obvious. This test clearly demonstrates high capabilities of the optical method for the erosion rate evaluation.

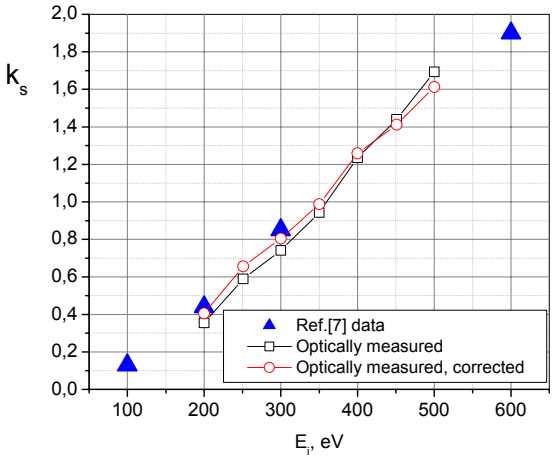

Figure 6. Comparison of the optically measured energy dependence of the chrome sputter coefficient with Ref.6 data.

3. Validation of the Optical Diagnostic Method Through Measurement of a Sample Sputter Coefficient Variation in the TAL Plume at Different Flow Rates

Similarly to the voltage dependence tests, variation of the SETAL erosion rate under varying xenon flow rate showed expected behavior on a qualitative level: the erosion rate grew with the rise of the flow rate through the thruster, due to the increased power of ion flux impinging the walls of the thruster discharge chamber. However accurate measurement of the ionic flux density at the discharge chamber wall represents a big problem. Therefore, measurement of sputter coefficient variation was implemented on a stainless steel sample located in the TAL plume, the same way as in the voltage variation experiment. Chrome sputter coefficient may easily be reduced from these measurements and compared with trivial predictions. At constant operating parameters, when only xenon flow rate changes, formulas (3) and (4) may be applied for the erosion rate sputter coefficient variations. If propellant utilization is assumed to be constant too, both variation of the xenon ion number density and ion beam current in formula (4) should be proportional to the flow rate variation and expression for the sputter coefficient variation takes a form:

$$\delta k_s = \frac{\delta R}{\delta j_+} \approx \frac{\delta N_+}{\delta j_+} \cdot \frac{\delta I_s}{\delta I_+} = \frac{\delta I_s}{\delta I_+} \tag{5}$$

Table 3 represents relative variation of the sample erosion rate and Cr sputter coefficient measured at three different flow rates.

Table 3. Variation of the TAL erosion rate and Cr sputter coefficients measured by optical method.

Flow rate, mg/s	Relative variation of the sample erosion rate	Relative variation of the Cr sputter coefficient
3.5	0.51	0.93
4.7	0.89	1.2
6.5	1	1

Ideally, the sputter coefficient in the last column of Table 3 should stay constant, because the ion beam energy was assumed to be constant in the tests. Apparent variation of the sputter coefficient in Table 3 may be attributed to limitations of equations (3) and (5), which assume constant ratio of excitation functions $\frac{Q_s}{Q_+}$ (see equation (2)). In the meantime, electron temperature T_e in the plume near the sample slightly varied in that experiment. The temperature was monitored through analysis of IR spectra by optical diagnostic method discussed in Ref.2. Despite that T_e variation was very small (within 0.2 eV) even that small variation might change the $\frac{Q_s}{Q_+}$ ratio. Reason for that is the big difference between excitation thresholds of the impurity emissions (3-5 eV) and xenon ionic emissions (14-16 eV). When electron temperature is 2-3 eV like in the TAL plume at a distance 0.5 m from the thruster, even small variation of the temperature becomes very critical for excitation of the Xe ionic lines. Formula (2) should be corrected in this case to take variation of the excitation function ratio into account. Note, that similar effect may be found in the discharge region too. However it is much weaker there, because electron temperature in the discharge may reach value of some tens of eV.

Given the arguments reasoning deviation of the reduced variation of the sputter coefficient, one may conclude that flow rate test once again demonstrated good capability of the optical diagnostic method for the erosion rate evaluation.

4. Effect of the Magnetic Field Variation

It is well known, that magnetic field intensity and configuration affect onto the plasma discharge properties and, in particular, to ion beam divergence in the TAL. Optimal values of the currents in the magnetic field system coils exist for each operating voltage and flow rate. At these values magnetic field configuration ensures highest efficiency and performance characteristics of the thruster. It has been shown before[8], that reducing of the currents below optimal values leads in increase of the ionic beam divergence and as the result - to increase of the thruster body erosion. This effect has been manifested by optical method in numerous tests. The erosion rate rose from factor of 2 to order of magnitude, depending on the current reduction in the coils of the magnetic field system.

From the other side when currents in the coils increase over the optimal values, magnetic field rises and the thruster departs away from the point of high efficiency operation. Power of high frequency oscillations in the discharge plasma increases in these conditions and the plasma particles have better chances to collide with the thruster body. Erosion rate must also increase in this situation. This effect has also been observed through real time measurement of the erosion rate variation by optical method. Table 4 demonstrates results of the measurements.

Table 4. Variation of the SETAL erosion rate caused by deviation of the currents in the magnetic field system coils from optimal values.

Configuration	Operating voltage, V	Operating current, A	Inner coil current, A	Outer coil current, A	Relative erosion rate
Optimal magnetic field	300	4.4	0.94	0.88	1
Lower magnetic field	300	4.75	0.46	0.31	7.5
Higher magnetic field	300	4.75	1.85	1.5	2.8

C. Temporal Variation of the Erosion Rate Value at the Moment of the TAL Operation Start-up.

Small growth of the erosion rate followed by its return to a stable level was observed during SETAL ware tests (see Figure 5 around 45th-55th hrs) upon the thruster start-up after temporal terminations. Operating parameters didn't change during the termination, so basically one might suppose that erosion rate must be the same before and after the terminations. To make sure that the erosion rate variation was not incidental and was not related to the optical method limitations a set of dedicated experiments was carried out. During those experiments the SETAL operation was terminated for a while and erosion rate was measured before and right after the terminations. The measurements were made at various operating regimes of the SETAL. Duration of the terminations also changed in different tests from seconds to hours. Analysis of the experimental data showed that basically the erosion rate temporal variation after the motor start-up reproduced itself from one test to another. Typical time history of the erosion rate variation is given in Figure 6.

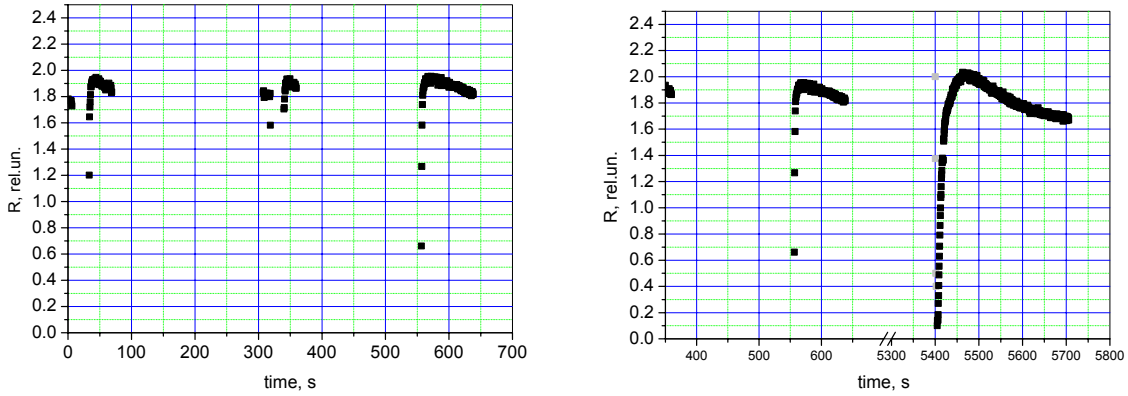

Figure 6. Temporal behavior of the SETAL relative erosion rate during termination of its operation.

Data points in the figure represent particular measurements, which were made with time step of one second. The erosion rate grew after the motor start-up to the value exceeding the prior termination level at about 5-10% and then it smoothly went down back to this level. As Figure 6 demonstrates, time interval where the erosion rate changes depends on the length of the pause in the thruster operation. One might suggest that discharge plasma properties, electron temperature in particular, vary during the thruster start-up and formula (3) may be not accurate at these conditions. However, time scale for the plasma properties variations is much smaller. Scrupulous analysis of the discharge spectra showed that intensities of all XeI, XeII and XeIII emissions were almost the same before and after the termination. So, by no way the electron temperature and plasma major specie number density could change and formula (3) must be appropriate to this case. Evidently, that observed variation of the erosion rate should be attributed to real processes taking place in the discharge plasma during the thruster start-up. One of these processes - sputtering of thin impurity films re-deposited onto various parts of the thruster body during preceding operation. Among other processes variation of sputter coefficient with surface temperature, changes of the surface roughness and/or material microstructure under ion bombardment and presence of organic films (oil) covering the thruster elements should also be mentioned. Additional study has to be undertaking for detailed explanation of the observed behavior of the erosion rate.

IV. Conclusions

The real time optical diagnostic method for evaluation of the TAL erosion rate variation has been elaborated and verified in dedicated tests. Comparison of the erosion rate measurements by the optical method with the data obtained in accelerated ware tests revealed good capabilities of the method. Results of relative variation of the thruster erosion rate from high-voltage to double-stage and high-current mode are agreed within 10-15% between optical method and ware tests. Measurements of the erosion rate of samples exposed by energetic ion beam in the TAL plume have also lead in predicted results. Conclusion can be derived from the method verification tests that semi-empirical formula (3) may be applied for reducing the erosion rate variation from experimental data in various cases of particular interest. However, variations of electron temperature in the TAL discharge plasma may affect

accuracy of formula (3). In this case, more general expression (2) must be utilized. Variations of electron temperature and excitation functions should be carefully monitored in the latter case.

Effect of the thruster erosion rate variation with magnetic field may be qualitatively explained by variation of the ion beam divergence and changing stability of the plasma discharge. Optimal magnetic field configuration exists where the erosion rate value is minimal. Departure of the magnetic field intensity from the optimal value causes the erosion rate increase.

Influence of temporal termination onto the thruster erosion rate may also be explained by real processes taking place in the thruster discharge. Effect of the temporal variation of the erosion rate after the thruster start-up has not been studied so far. So, no reliable data are available to compare with the optical method results.

Future efforts should be addressed to calibration of the optical method to make it capable measuring absolute value of the erosion rate. Also, utilization of LIF technique for measurements of the impurity species content and velocity would make a real sense to improve accuracy of the method.

Acknowledgment

This work has been accomplished within the frame of CRDF CGP Award RP2-2370-KO-02. CRDF Project Manager was Mr.W.Freeman.

References

[1] M.T.Domonkos, R.E.Stevens, "Assessment of Spectroscopic, Real-Time, Ion Thruster Grid Erosion Rate Measurements", *36th AIAA JPC,* AIAA 2000-3815, July, 2000, Huntsville, Alabama.

[2] G.Karabadzhak, "Improvement of Optical Diagnostic Technique for a Xenon Operating Hall Effect Thruster", *4th International Spaccraft Propulsion Conference*, June, 2004, Sardinia, Italy

[3] G.Karabadzhak, A.Semenkin, S.Tverdokhlebov, "Semi-empirical method for evaluation of a xenon operating Hall thruster erosion rate through analysis of its emission spectra," *Proc. 3rd International Conference on Spacecraft Propulsion*, Cannes, France, October, 2000, p.909-912.

[4] G.Karabadzhak, A.Semenkin, S.Tverdokhlebov, "Evaluation of a Xenon Operating Hall Thruster Body Erosion Rate Through Analysis of its Optical Spectra", *37th Joint Propulsion Conference,* paper AIAA-2001-3889, Salt Lake City, 2001.

[5] D.Pagnon, P.Lasgorceix, M.Touzeau, "Control of the Ceramic Erosion by Optical Emission Spectroscopy: Results of PPS1350-G Measurements", *4th International Spacecraft Propulsion Conference*, June, 2004, Sardinia, Italy.

[6] Pleshvtsev, N.V., *Sputtering processes*, Moscow, 1968 (in Russian).

[7] Zakharenkov L.E., Lebedev Yu.V., Semenkin A.V., "Diagnostic particularities and results of measurements of local plasma parameters of anode layer thrusters", *Kosmonavtika i raketostroenie*, 1(34), 2004, pp. 14-34.

[8] Semenkin A.V., et al, "Development program and Preliminary Test Results o the TAL-110 Thruster", AIAA-99-2279, *35th AIAA/ASME/SAE/ASEE Joint Propulsion Conference*, June 20-24, 1999, Los Angeles.